Journal of Applied Polymer Science

Evaluation of a new water-compatible hybrid molecularly imprinted polymer combined with restricted access for the selective recognition of folic acid in binding assays

Fernanda Midori de Oliveira,[1] Mariana Gava Segatelli,[1] César Ricardo Teixeira Tarley[1,2]

[1]Departamento De Química, Universidade Estadual De Londrina, Rod. Celso Garcia Cid, PR 445 Km 380, Campus Universitário, Londrina, PR, CEP 86051-990, Brazil

[2]Departamento De Química Analítica, Instituto Nacional De Ciência E Tecnologia (INCT) De Bioanalítica, Universidade Estadual De Campinas (UNICAMP), Instituto De Química, Cidade Universitária Zeferino Vaz S/N, Campinas, SP, CEP 13083-970, Brazil

Correspondence to: C. R. T. Tarley (E-mail: ctarleyquim@yahoo.com.br)

ABSTRACT: This article deals with the synthesis of an organic−inorganic hybrid molecularly imprinted poly(methacrylic acid-trimethylolpropane trimethacrylate)/SiO_2 combined with restricted access. Fourier Transform Infrared Spectroscopy, Transmission Electron Microscopy, Thermogravimetric Analysis, and textural data were used to characterize the structure of material. Higher selectivity was obtained for the molecularly imprinted polymer with restricted access when compared to nonimprinted polymer with restricted access, confirming the imprinting effect. The folic acid sorption for the polymers molecularly imprinted with restricted access, nonimprinted with restricted access, and molecularly imprinted, exhibited the following values of 5.6, 4.5, and 4.8 mg g^{-1}, respectively. Kinetic experimental data were very well adjusted to Elovich and pseudo-second-order models, which suggest that the sorption of folic acid takes place in binding sites with different energies. The obtained values of enthalpy, entropy and Gibbs free energy of −12.79 kJ mol^{-1}, −36.38 K^{-1} J mol^{-1}, and −1.76 kJ mol^{-1}, respectively, showed that the sorption of folic acid onto molecularly imprinted polymer combined with restricted access occurs spontaneously, is of both exothermic and of physical nature with an increase of ordering at the solid−solution interface. © 2016 Wiley Periodicals, Inc. J. Appl. Polym. Sci. **2016**, *133*, 43463.

KEYWORDS: applications; adsorption; hydrophilic polymers; kinetics

Received 13 September 2015; accepted 24 January 2016

DOI: 10.1002/app.43463

INTRODUCTION

Since its first synthesis 5 decades ago, molecularly imprinted polymers (MIPs) have been ideally designed to produce materials with specific recognition site for a predetermined target molecule with a wide range of application, including development of electrochemical and optical sensors, separation techniques, controlled drug delivery system, methods for sample preparation and catalysts.[1–7] Despite the outstanding features of MIPs, very well documented in the field of molecular recognition, there are still some difficulties in their synthesis which must be addressed. For instance, it is very well known that the higher molecular recognition of MIPs towards the template molecule occurs in a solvent with physical and chemical properties very similar to a porogenic solvent used for their preparation. Therefore, as the MIPs are usually prepared in relatively nonpolar solvents as porogenic solvent, their practical application in aqueous environment fail to exhibit specific template binding, most likely due to nonspecific interactions between template molecule and binding sites of polymer, due to the presence of hydrophobic bonds[8,9] and cross-reactivity for compounds structurally similar to the template molecule.[10] Additionally, the direct application of MIPs for the extraction of analyte from environmental water samples or biological fluids can be drastically affected by irreversible adsorption of larger molecules onto MIP surface, such as proteins, carbohydrates, and humic and fulvic acids.[11,12] Another issue related to challenges in obtaining selective MIPs relies on the size of the target molecule. In general, the use of larger target template makes very difficult a better control of the orientation and density of binding sites by means of interaction of functional monomer, which justifies the very few studies on this subject. In addition, upon polymerization, the mass transfer of template towards the binding sites can also be diminished due to the large size of the molecule.[13] Therefore, new approaches are needed and are being increasingly developed for suppressing the drawbacks aforementioned regarding the performance of MIPs. Inorganic molecularly imprinted polymers prepared by means of sol−gel process have

been very efficient for the application of MIPs in aqueous environment once the oxide network is created by hydrolysis and polycondensation reactions of molecular precursors, usually in polar solvent in presence of water.[14,15] Surface molecular imprinting on the surface of substrate is considered an interesting approach for solving the problems of mass transfer and accessibility of large molecules towards the surface of MIP.[16,17] For the organic molecularly imprinted polymers, the use of hydrophilic comonomers, such as 2-hydroxyethyl methacrylate (HEMA) and glycerol dimethacrylate (GDMA), into the molecular imprinting system has been recently reported for the hydrophilic modification of polymeric surface with pendant hydroxyl groups and, as a consequence, providing water-compatibility to MIP.[18–20] These materials are also designed as restricted access material-molecularly imprinted polymer (RAM-MIP) due to the exclusion properties of macromolecules. Since the hydrophilic surface of MIP and macromolecule are both polar, the presence of water at the interface of this system prevents or diminishes the adhesion of macromolecules.[21] Although RAM-MIP synthesized with hydrophilic comonomers is particularly well-suitable for applications in aqueous medium, the presence of hydroxyl groups from comonomers may decrease the formation of imprinting sites as a result of interaction with template molecule by means of hydrogen bonds. In this sense, the use of comonomers containing epoxy ring, such as 3-(glycidyloxypropyl)trimethoxysilane (GPTMS) and glycidyl methacrylate (GMA) as pro-hydrophilic comonomer seems to be an ideal way for obtaining water-compatible RAM-MIP with better selectively since the epoxy ring interferes less in the pre-polymerization complex formation between monomer and template molecule. The former comonomer has been used to obtain water-compatible RAM-MIP in the extraction of p-acetaminophenol from water samples.[22] In this study the epoxy ring was opened upon polymerization using diluted mineral perchloric acid providing hydrophilic modification on the surface of RAM-MIP.

As evidenced, some efforts have been performed to obtain new RAM-MIP, but the number of studies on this subject is still scarce. In this sense, our proposal is to synthesize a new organic−inorganic hybrid molecularly imprinted poly(methacrylic acid-trimethylolpropane trimethacrylate)/SiO_2 combined with restricted access (RAM-MIP) as a selective sorbent for a larger target molecule, folic acid in this case, using 3-(glycidyloxypropyl)trimethoxysilane as pro-hydrophilic comonomer. In this strategy, we have combined the advantages of comonomers using the epoxy ring instead of those containing hydroxyl groups together with the interesting properties of hybrid materials. So far, at the best of our knowledge, hybrid molecularly imprinted polymers with restricted access have not yet been synthesized. It has been very well documented that these organic−inorganic hybrid materials fabricated by incorporation of template molecules into rigid inorganic or inorganic organic networks give rise to materials with complementary properties to that observed by isolated organic or inorganic phase. Some characteristics of these materials can be cited, such as superior thermal stability, high hardness, good textural and morphological features and uniform particle sizes.[12,23–29] In this study, folic acid was chosen as target molecule considering its relatively large size, incipient data on literature regarding synthesis of MIP for this molecule, and due to its great clinical importance to human health as a water soluble vitamin. One should note that from a survey of literature some studies regarding synthesis of MIPs as adsorbents for folic acid have been reported, but neither of them makes use of hybrid molecularly imprinted polymers with restricted access. These previously published studies still involve the use of organic soluble analogues complementary to substructures of the folic acid as template or require complicated previous synthesis of trifunctional monomers.[13,30] Additionally, in some of them the batch partitioning experiments were performed in organic solvents, which demonstrate the absence of compatibility of the MIP in aqueous medium. Other publications addressed to the synthesis of MIP for folic acid and its application are devoted to the development of sensors, but the use of hybrid molecularly imprinted polymers with restricted access has not been investigated in these studies yet.[16,31–34] According to the aforementioned and bearing in mind that RAM-MIP and respective RAM-NIP (nonimprinted polymer) for folic acid were herein synthesized for the first time, these materials were characterized by TEM, TGA, FTIR, and nitrogen adsorption experiments by means of the physical adsorption. In addition, kinetic studies, selectivity studies for evaluating the recognition ability of RAM-MIP in discriminating structurally similar compounds, and studies concerning the ability of RAM-MIP in excluding macromolecules were performed.

EXPERIMENTAL

Chemicals and Materials

The chemicals methacrylic acid (MAA), trimethylolpropane trimethacrylate (TRIM), tetraethoxysilane (TEOS), 3-(glycidoxypropyl)trimethoxysilane (GTMS), vinyltrimethoxysilane (VTMS), 2,2-azoisobutyronitrile (AIBN), folic acid (FA), caffeine (CAF), acetaminophen (AC), 4-aminobenzamide (ABA) were purchased from Sigma-Aldrich® (Steinheim, Germany). The solvents (acetonitrile and methanol) and acids (hydrochloric acid and acetic acid) were purchased from Sigma-Aldrich® (Steinheim, Germany). Potassium hydroxide was purchased from Vetec® (São Paulo, Brazil). All the reagents were used without prior purification.

Instruments

The infrared spectra were obtained with a Fourier Transform Infrared Spectrometer, Shimadzu® model FTIR 8300 (Kyoto, Japan). Infrared (IR) transmission spectra (KBr pellets) recorded between 4000 and 400 cm^{-1} were used to elucidate functional groups present in the polymers. The pH measurements were performed using pH meter Metrohm® 827 (Herisau, Switzerland). A UV-Vis spectrophotometer Perkin-Elmer® Lambda 25 (MA, USA) was employed for the measurements in the ultraviolet-visible region. The thermal analysis was carried out by a thermogravimetric analyzer Perkin-Elmer® TGA 4000 (MA, USA) with temperature variation from 30 to 900 °C at a heating rate of 10 °C min^{-1}. The surface area, pore size, and pore volume were determined from nitrogen adsorption using a Quantachrome® Nova 1200e (Boynton Beach, USA). The

samples were heated at 85 °C under vacuum for 5 h, then submitted to nitrogen gas adsorption, and the BET model (Brunauer, Emmett, Teller) was applied to the data obtained for determination of surface area, and the BJH model (Barrett, Joyner, Halenda) for determination of pore size and pore volume. The transmission electron microscopy images were taken using a microscope JEOL® JEM-1400 with an accelerating voltage of 120 kV. The samples were previously dispersed in ethanol with sonication for 20 min and then the suspension was dripped on copper grids and dried under vacuum. The study of the thermodynamic constants was performed using a thermostatic bath Marconi® MA-184 (Piracicaba, Brazil) at temperatures ranging from 303.15 to 353.15 K. In order to evaluate the reusability of RAM-MIP a SPE (solid phase extraction) procedure was performed using a manifold system (Bio-Rad) coupled to a vacuum pump (Marconi MA2057), whose eluates were analyzed using a HPLC system series LC-20AD/T LPGE KIT consisting of CLC-ODS column (250 mm × 4.6 mm id, 5 μm in particle size) and a guard column Phenomenex (4.0 mm × 3.0 mmm i.d., 5 μm in particle size), a 7725i manual injector with a 20 μL loop, (Rheodyne®, CA, USA), a CTO-10AVP column oven and a LC-20AT controller chromatographic separations were carried out using a Shimadzu® (Kyoto, Japan). The peak purity was determined on a photodiode-array detector (PDA) and monitored at λ_{max} 281 nm. Chromatographic separation was performed in gradient mode using the mobile phase acetonitrile (A) and 0.266 mol L^{-1} acetate buffer pH 5.7 (B). The separation was started with 15% A with gradient up to 24% A in 8.5 min, being the composition maintained until the final the analysis.

Synthesis of Hybrid Molecularly Imprinted Polymer with Restricted Access (RAM-MIP)

The synthesis of the polymers consisted of the use of the following reagents: folic acid (template), methacrylic acid (functional monomer), trimethylolpropane trimethacrylate (crosslinking agent), vinyltrimethoxysilane (coupling agent), tetraethoxysilane (inorganic precursor), and (3-glycidyloxypropyl)trimethoxysilane (comonomer), in the following amounts 2.0 mmol (0.88 g); 12.0 mmol (1.03 g); 24.0 mmol (8.12 g); 2.9 mmol (0.43 g); 52.0 mmol (10.83 g), and 48.0 mmol (11.34 g), respectively. The polymer synthesis procedure was carried out by FA solubilization in HCl with mechanical stirring for 30 min. Then 310.0 mL of acetonitrile and MAA were added, and subjected to mechanical stirring for 30 min. Thereafter TRIM, VTMS, and 600 mg of AIBN were added. Next, nitrogen gas was bubbled into the solution for 5 min and the flask was sealed. The mixture was polymerized at 60 °C for 24 h in an oil bath. The polymer obtained was filtered under vacuum and dried for 24 h at 60 °C. This material was named poly(MAA).

In the next step, 10.054 g of the organic polymer obtained was resuspended in 300.0 mL of ethanol by mechanical stirring. In sequence, TEOS, GTMS, and 26.0 mL of 1.0 mol L^{-1} NaOH were added. The mixture was polymerized for 24 h at room temperature under mechanical stirring. After this time, the material obtained was filtered under vacuum and dried for 48 h at 60 °C. This material was named poly(MAA)-SiO_2 1.[35,36] For the epoxy ring opening, 10,000 g of poly(MAA)-SiO_2 1 was mixed with 500.0 mL of 0.18 mol L^{-1} HCl, which remained under stirring at 60 °C in an oil bath for 36 h, and then was filtered under vacuum and dried at 60 °C. This material was named poly(MAA)-SiO_2 2.[37] The template extraction was performed with methanol:-acetic acid (90:10, v/v) using a Soxhlet system. This material was named RAM-MIP. The same methodology employed for the synthesis of RAM-MIP was used for the MIP, except by the use of GTMS. RAM-NIP material was also prepared and, in this case, folic acid was not used in the synthesis. Figure 1 depicts the schematic representation of the RAM-MIP synthesis.

pH Optimization and Sorption Kinetics

The pH values were evaluated in a range of 1.5 − 10.4, in order to check the influence of this variable on the sorption of folic acid by RAM-MIP. For this study, the following buffers were used: KCl/HCl (pseudo buffer for pH 1.5), acetate (pH 4.4 and 5.4), phosphate (pH 6.4 and 7.4) and ammoniacal (pH 8.4, 9.4, and 10.4), all in the concentration of 0.01 mol L^{-1}. The experiments were carried out in batch mode by using 50 mg of RAM-MIP stirred at 120 rpm using mechanical stirring for 60 min with 40.0 mL of a 10 mg L^{-1} folic acid solution. Then, the mixture was centrifuged and the supernatant was filtered in 0.45 μm Nylon® syringe filter and analyzed by UV-Vis spectrophotometry at a wavelength of 281 nm. The influence of the time on the sorption profile from RAM-MIP, RAM-NIP, and MIP, followed the same methodology as for pH optimization studies, but with pH fixed at 1.5. The stirring times were varied from 1 up to 720 min.

Thermodynamic Parameters

In order to estimate the energies related to folic acid sorption process in RAM-MIP, enthalpy (ΔH), entropy (ΔS), and Gibbs free energy (ΔG) of the system were calculated. The thermodynamic study of folic acid sorption process in the RAM-MIP was carried out under mechanical stirring at 120 rpm of 50 mg of RAM-MIP with 40 mL of a folic acid solution for 390 min at temperatures ranging from 303.15 to 353.15 K using thermostatic bath. Then, the mixture was filtered in 0.45 μm Nylon® syringe filter and analyzed by UV-Vis spectrophotometer at a wavelength of 281 nm.[38] The enthalpy and entropy were obtained from the intercept and slope of the graph of $\ln K_d$ versus $1/T$ (Van't Hoff plot), according to the eq. (1). The distribution coefficient (K_d) in different temperatures was obtained by dividing sorption amount (Q_e, mg g^{-1}) and the supernatant concentration (C_e, mg L^{-1}), R is the universal gas constant ($R = 8.314$ J mol^{-1} K^{-1}) and T is the temperature in Kelvin.[38,39]

$$\ln K_d = -\frac{\Delta H}{R}\left(\frac{1}{T}\right) + \frac{\Delta S}{R} \quad (1)$$

The Gibbs free energy of the system was determined using the eq. (2) in the temperature of 303.15 K.

$$\Delta G = \Delta H - T\Delta S \quad (2)$$

Selectivity Parameters

In order to evaluate the effective formation of selective cavities for folic acid during synthesis of RAM-MIP, competitive binding assays were carried out using folic acid, 4-aminobenzamide (ABA), acetaminophen (AC) and caffeine (CAF). Binary solutions of folic acid and the competitor, both at a concentration of 10 mg L^{-1} were stirred with 50 mg of RAM-MIP of RAM-NIP for 390 min (equilibrium time) at 120 rpm. After stirring,

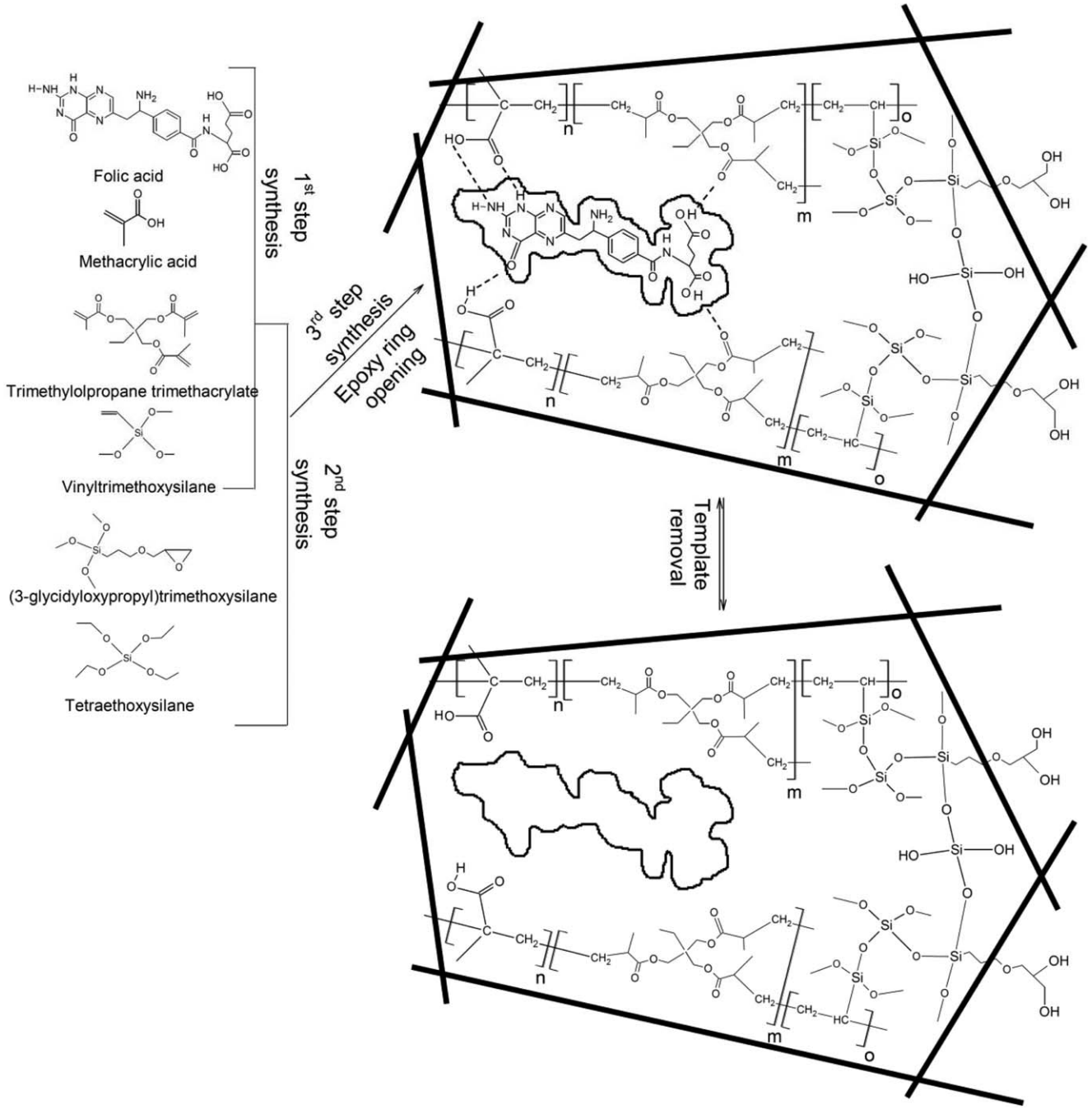

Figure 1. Schematic representation of the RAM-MIP synthesis.

the solutions were centrifuged, filtered through a 0.45 μm Nylon® membrane and analyzed in UV-Vis spectrophotometer. The wavelengths used were 221 nm (ABA), 243 nm (AC), and 272 nm (CAF), with subsequent deconvolution of the spectra obtained. The distribution coefficient (K_d), selectivity coefficient (k), and relative selectivity coefficient were calculated according to literature data.[40]

Swelling Analysis

The swelling ratio (Sr) of each polymer, RAM-MIP, RAM-NIP, and MIP was determined to evaluate the hydrophilicity of materials by determining the water uptake. For this study, 100 mg of each polymer (dry mass) was mechanically stirred with 10 mL of ultrapure water during 24 h, and then the materials were filtered in 0.45 μm Nylon® membrane under vacuum and weighed (wet mass). The initial and final masses of polymers were used to calculate the swelling ratio (Sr) determined by eq (3).[41]

$$\text{Swelling ratio (Sr)} = (\text{Wet mass} - \text{Dry mass})/(\text{Dry mass}) \times 100\% \quad (3)$$

RESULTS AND DISCUSSION

Characterization of Materials by Infrared Spectroscopy and Thermogravimetric Analysis

The RAM-MIP and the polymers obtained in each synthesis step were characterized by infrared spectroscopy to verify the presence of functional groups (Figure 2) and by thermogravimetric analysis to monitor changes in thermal stability (Figure 3). In all FTIR spectra, the presence of a wide and intense band at 3460 cm^{-1}, ascribed to the stretching of the O—H bond, present in folic acid and methacrylic acid was observed. The signals at 2968 and 1465 cm^{-1} are assigned to the asymmetric stretching of CH_2 present in TRIM and VTMS structures. The peak at 1729 cm^{-1} is attributed to stretching C=O of FA, MAA, and TRIM. In 1634 cm^{-1}, the residual C=C stretch of MAA and TRIM is observed. The signal attributed to angular deformation out of plane of CH_3 (umbrella) present in TRIM and VTMS can be observed in 1388 cm^{-1}. The peaks at 1265 and 1161 cm^{-1} are present in FA and MAA and can be attributed to the stretching of group COOH and O-C(O)-C, respectively. The deformation of N—H bond of the primary amine present in the structure of folic acid was observed at 1564 cm^{-1}.[42] The bands at 1062 and 466 cm^{-1} are ascribed to Si—O—Si and Si—O stretching, which proves the hydrolysis and condensation of the inorganic fraction, and it can be observed that the poly(MAA) does not show these two bands.[23,43] According to Figure 2(B), the spectra of RAM-MIP and RAM-NIP were very similar, which confirms the removal of template from the polymeric matrix. The spectrum of MIP was somewhat different from the other ones, especially by the pronounced signal in the region of 1087 cm^{-1} assigned to the inorganic Si—O—Si group. This higher signal can be ascribed to the absence HCl in the synthesis, which avoids the hydrolysis of Si—O—Si group and, as a consequence, gives rise to a higher amount of inorganic fraction in the MIP. This finding was further confirmed by thermogravimetric analysis, where a higher ceramic yield was observed for MIP.

The polymerization of silica fraction was also confirmed by thermogravimetric analysis due to lower ceramic yield which poly(MAA) presented in relation to poly(MAA)-SiO_2 1,

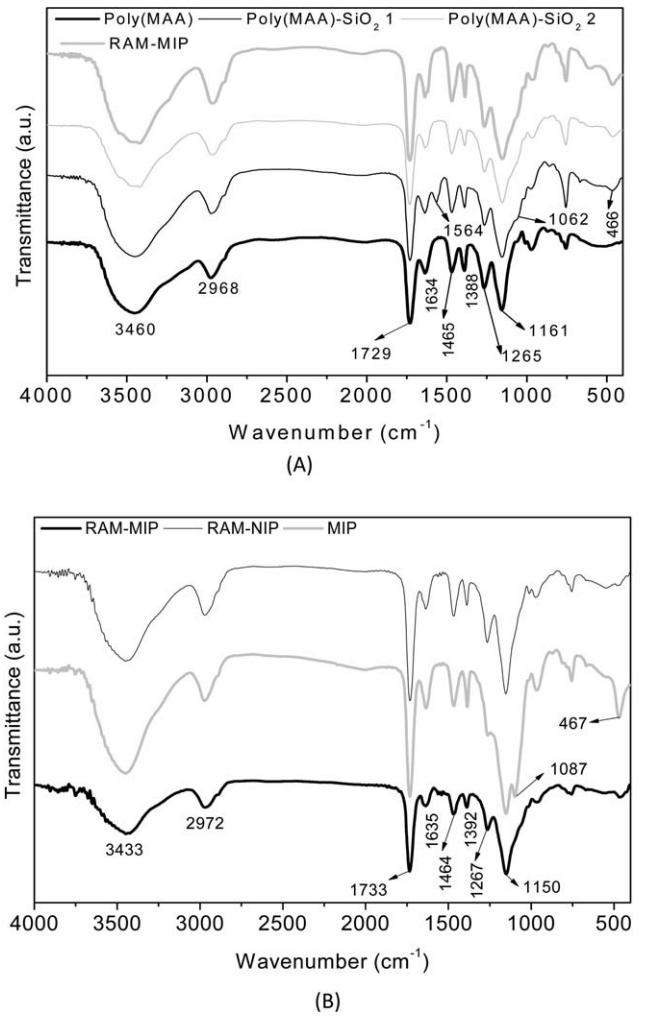

Figure 2. FTIR spectra of (A) RAM-MIP and polymers obtained in different stages of synthesis (B) RAM-MIP, RAM-NIP, and MIP.

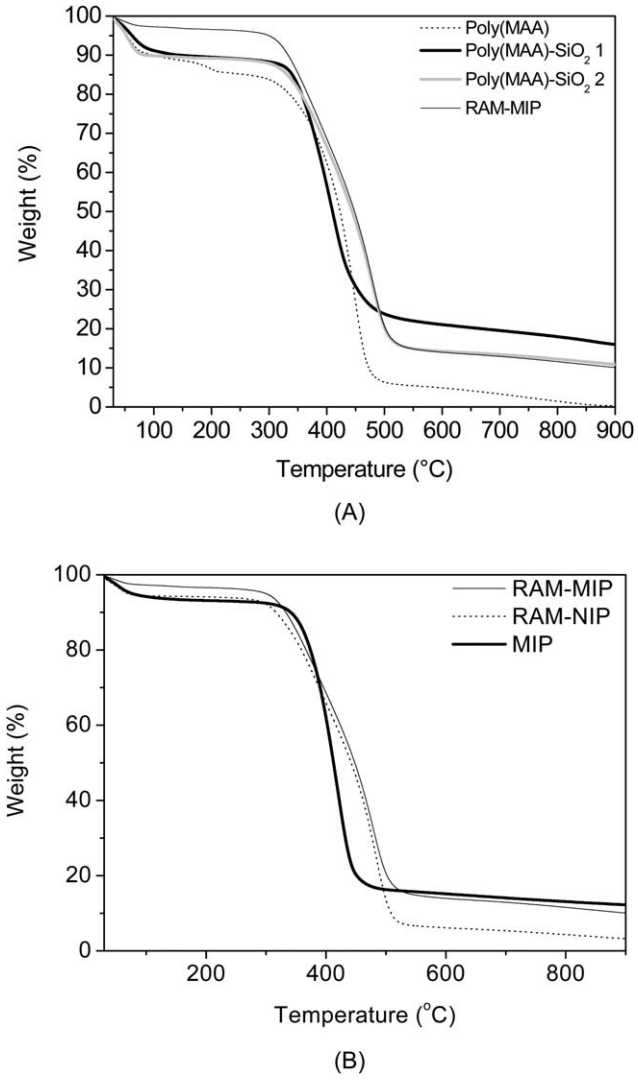

Figure 3. Thermogravimetric curves of (A) RAM-MIP and polymers obtained in different stages of synthesis (B) RAM-MIP, RAM-NIP, and MIP (B).

poly(MAA)-SiO_2 2, and RAM-MIP [Figure 3(A)]. RAM-MIP showed lower thermal stability when compared with the polymers obtained in the synthesis steps, according with the temperature onset values (T_{onset} is the point of intersection of the extrapolated baseline with the tangent of the curve slope).[44] The values of T_{onset} obtained were 334, 348, 336, 317 °C for poly (MAA), poly(MAA)-SiO_2 1, poly(MAA)-SiO_2 2, and RAM-MIP, respectively. The relative low thermal stability of RAM-MIP can probably be related to the removal of folic acid from polymeric matrix, with consequent weakening of the chemical bounds in the chain segments due to absence of stable interactions of FA with the functional monomer. In addition, from Figure 3(A), it is possible to observe weight loss in ~55 °C due to loss of the physically adsorbed water. The thermogravimetric curve of poly (MAA) showed weight loss (3.9%) at 203 °C, related to the dehydration of the functional monomer and the maximum degradation rate with weight loss of 79.7% at 449 °C, attributed to the decomposition of chain segments. Regarding the poly(MAA)-SiO_2 1, the maximum degradation rate was observed at 410 °C with weight loss of 69.2%, which is associated with degradation of the polymer chain segments.[23] The materials poly(MAA)-SiO_2 2 and RAM-MIP have very similar thermogravimetric curves with weight loss of 23.9 and 26.9% at 379 and 356 °C, respectively, which can be related to the degradation of GTMS. These materials also exhibited maximum degradation rate of chain segments at 480 °C.[45,46] A comparison of thermal behavior of RAM-MIP, RAM-NIP, and MIP was also evaluated. As observed from Figure 3(B), the T_{onset} were found be 317, 311, and 351 °C for RAM-MIP, RAM-NIP, and MIP, respectively. The higher thermal stability of MIP regarding RAM-MIP and RAM-NIP can be explained due to either absence of GTMS or absence of HCl in the synthesis process, thus making the whole chain stiffer.

Morphological and Textural Characterization of Polymers

The transmission electron microscopy images (Figure 4) were obtained in order to evaluate the morphology and the presence of phase's separation of organic and inorganic matrices in the polymers. It was observed a high adherence between the particles of polymer with morphological properties of monoliths, which is a very interesting feature for the use of these materials for packing columns in the solid phase extraction procedures. From the RAM-MIP and RAM-NIP images, it is possible to visualize a typical surface of the silica matrix, which clearly demonstrates the formation of a hybrid material.[47] The morphology of poly (MAA) [Figure 4(A)] was substantially different from those ones obtained for the hybrid materials, which shows again the polymer network between organic and inorganic phases. On the other hand, the morphology of MIP was different from those ones obtained for the hybrid materials, but slightly similar to that one observed for the poly(MAA) and with irregular particle sizes. This finding can be attributed to the absence of the GTMS in the synthesis of both MIP and poly(MAA). As it is very well known, the GTMS is considered a crosslinking agent of polymeric network and, as a consequence, its absence in the synthesis may hinder the formation of uniform particle sizes.[48,49]

The results of surface area, average pore diameter and pore volume are shown in Table I. Comparing the results obtained, it is

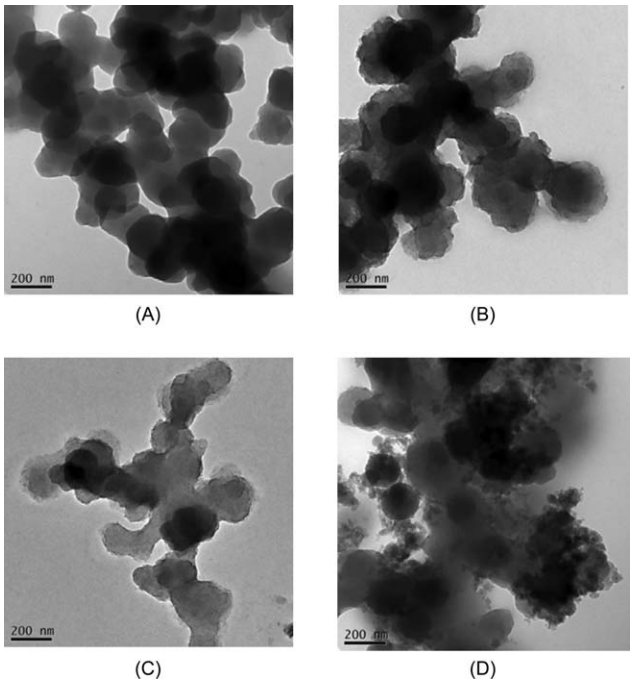

Figure 4. Transmission electron micrographs (A) poly(MAA), (B) RAM-MIP (C) RAM-NIP, and (D) MIP.

observed that the RAM-MIP has low surface area and low pore volume in relation to the RAM-NIP. The explanation for this morphological difference may be related to the presence of the template in the polymerization, which may increase the solubility of the monomer-template complex in the solvent.[50] As a consequence; it hinders the porogenic solvent removal of the polymer interstices, obtaining smaller pores and, in consequence, smaller surface area. In regard to MIP, the RAM-MIP has a smaller surface area and lower pore volume possibly due to the modification with the GTMS molecule that can occupy the inside of the pores of the polymer and thereby decrease the pore volume and surface area. However, despite having lower surface area and pore volume, the RAM-MIP has a higher sorption capacity of folic acid in relation to RAM-NIP and MIP, as will be seen in the sorption kinetics study. The pore size obtained from these materials can be classified according to the IUPAC as mesoporous materials by having pore size between 2 and 50 nm.[51]

pH Optimization and Sorption Kinetics

The time effect on the sorption of folic acid by polymers RAM-MIP, RAM-NIP, and MIP were studied with mechanical agitation. The pH used in this study was 1.5, because in previous

Table I. Textural Data of Surface Area, Pore Volume, and Pore Size

Polymer	Surface area ($m^2\ g^{-1}$)	Pore volume ($cm^3\ g^{-1}$)	Pore size (nm)
RAM-MIP	17.5	0.039	3.04
RAM-NIP	61.0	0.114	3.32
MIP	55.3	0.103	3.35

studies carried out in a pH range from 1.5 to 10.4 (data not shown) it was observed that acid medium favors the sorption of folic acid in the RAM-MIP. The higher sorption observed at pH 1.5 occurs due to the protonation of the functional monomer (pKa 4.46),[52] which favors the formation of hydrogen bonds and dipole−dipole momentary and permanent interactions between the functional groups present in the AF and MAA.[30] Thus pH 1.5 was used in subsequent studies.

In the kinetics sorption studies (Figure 5) it was observed that the time required to reach the equilibrium of folic acid between the solid phase and the liquid phase was found to be 390, 180, and 120 min, respectively, for RAM-MIP, RAM-NIP, and MIP. These results can be attributed to the morphological differences existing between the polymers. The RAM-MIP has a low surface area and smaller pore volume. These characteristics reduce the speed of mass transfer of folic acid towards the sorptive site in comparison with RAM-NIP and MIP.[53] Although the folic acid sorption in the RAM-MIP requires a higher equilibrium time, the sorbed amount was higher (5.6 mg g^{-1}) compared with the RAM-NIP (4.5 mg g^{-1}). In this case the higher folic acid sorption by the RAM-MIP is related to the greater affinity of the analyte for the selective cavity without dependence of textural data. The MIP, in turn, has cavities with an affinity for folic acid (selective cavities) and textural characteristics similar to the RAM-NIP. These two factors combined favor the obtaining of a lower equilibrium time, compared with the other polymers, as well as an intermediate sorption of 4.8 mg g^{-1}.[40] Another aspect that can be considered to justify the lower equilibrium time for the MIP, results in the absence of the surface modifier (GTMS) in the polymer matrix, which can act as a chemical barrier to the mass transport of the folic acid.

The following models were applied in the experimental kinetic data: pseudo-first-order, pseudo-second-order, Elovich and intraparticle diffusion[54] and the obtained results are shown in Table II. According to the linear correlation coefficients obtained as well as the Q_e predicted by models, it was verified that the pseudo-second-order, Elovich and intraparticle diffusion models fitted very well to the experimental kinetic data. The predicted sorption by the pseudo-second-order model was very similar to that obtained in the experimental data for all polymers evaluated. On the other hand, as observed from Table II, the Q_e predicted by the pseudo-first-order model was very different from the experimental data. The mathematical models adjusted to the experimental data indicate that RAM-MIP, RAM-NIP, and MIP present sites with different bond energies on the materials surface, which is also confirmed by the good adjustment of Elovich model.[55]

The intraparticle diffusion model presented three linear segments, but only the two ones are shown in Table II. The first one refers to quick analyte diffusion through external surface of sorbent. The second linear segment is related to the gradual intraparticle sorption of analyte into pores of the materials, while the third inclination is attributed to the equilibrium stage. According to Table II, it was observed that the C constant values, *i.e.,* the constant related to the thickness of the boundary layer (mg g^{-1}) in the first inclination for the three materials are

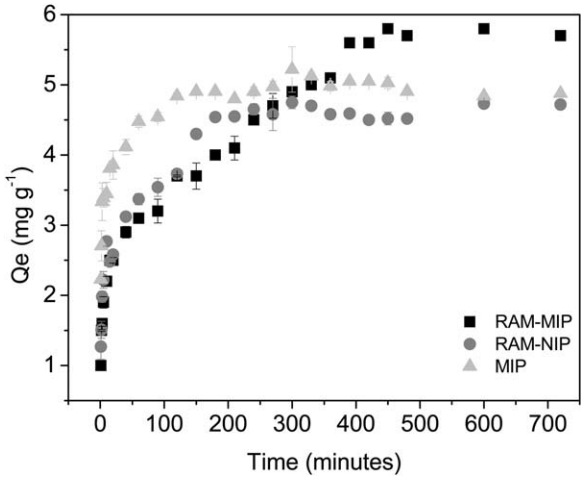

Figure 5. Sorptive profile of the polymers RAM-MIP, RAM-NIP, and MIP as time function.

different from zero, thus indicating that the sorption occurs by both intraparticle diffusion and sorption process in the external surface of polymers.[56–58]

Thermodynamic Parameters and Competitive Sorption for Assessing the Selectivity of RAM-MIP

The Van't Hoff plot was obtained from the linear relationship ln K_d versus $1/T$ giving rise to the following linear equation ln $K_d = 1538.13(1/T) - 4.38$ with linear correlation coefficient of 0.991. From the angular and linear coefficients of this equation, and by using the eq. (1), the ΔH and ΔS were, respectively determined as being 12.79 kJ mol^{-1} and -36.38 K^{-1} J mol^{-1}. Moreover, the Gibbs free energy of -1.76 kJ mol^{-1} at 303.15 K was determined by using the eq. (2). The negative enthalpy indicates that folic acid sorption onto RAM-MIP is exothermic, which implies that the sorption process is favored in lower temperatures, very characteristic of sorptive process of physical nature. Furthermore, the low enthalpy obtained (<40 kJ mol^{-1}) confirms that folic acid sorption on the surface of the RAM-MIP is of physical nature (physisorption). The interactions of physical nature involve intermolecular forces (Van der Walls forces), especially permanent and induced dipole−dipole with energy ranging from 2 to 29 kJ mol^{-1} and the analyte can establish interactions with more than one site along the surface of the polymer. This supposition is very plausible taking into account the chemical nature of folic acid and the binding sites of RAM-MIP. It must be emphasized that intramolecular hydrogen bonding between the binding sites of RAM-MIP with folic acid can also occurs, bearing in mind that this type of interaction involves low sorption energy (2 − 40 kJ mol^{-1}).[59] The negative entropy obtained for folic acid sorption in the RAM-MIP indicates that the sorption process decreases system disorder and the negative Gibbs free energy indicates a spontaneous process.[38,39]

Figure 6 shows the selectivity coefficient (k) for the RAM-MIP and RAM-NIP obtained from the binary competitive sorption FA/CA, FA/AC, and FA/ABA. The molecular structures of folic acid and competitors are depicted in Figure 7. The competitor molecules were chosen because they have similar structures to

Table II. Calculated Parameters for Pseudo-First-Order, Pseudo-Second-Order, Elovich and Intraparticle Diffusion Models

	Pseudo-first-order $\log(Q_e - Q_t) = \log Q_e - \frac{k_1}{2.303}t$			Pseudo-second-order $\frac{t}{Q_t} = \frac{1}{k_2 Q_e^2} + \frac{1}{Q_e}t$			Elovich $Q_t = \frac{1}{\beta}\ln(\alpha\beta) + \frac{1}{\beta}\ln t$			Intraparticlediffusion $Q_t = k_{id}t^{1/2} + C$		
Sorbent	k_1	Q_e	r	k_2	Q_e	r	β	α	r	K_{id}	C	r
RAM-MIP	0.01	3.85	0.99	0.01	5.05	0.99	1.53	1.77	0.97	0.41	0.82	0.97
										0.19	1.58	0.99
RAM-NIP	0.01	2.68	0.95	0.03	4.13	0.99	1.88	5.64	0.98	0.70	0.61	0.99
										0.20	1.74	0.99
MIP	0.02	1.79	0.95	0.09	4.60	0.99	2.10	84.86	0.97	1.49	0.69	0.98
										0.15	3.10	0.98

Experimental $Q_e = 5.6$ mg g^{-1} for RAM-MIP, 4.5 mg g^{-1} for RAM-NIP and 4.8 mg g^{-1} for MIP K_1: It is constant for pseudo-first-order of sorption process (min^{-1}); K_2: It is constant for pseudo-second-order of sorption process (g mg^{-1} min^{-1}); β: It associated with the surface coverage extension and the activation energy of chemisorption (g mg^{-1}); α: is the initial sorption rate constant (min^{-1} mg g^{-1}); K_{id}: is the coefficient of diffusion internal(mg g^{-1} min$^{-1/2}$); C: is a constant related to the thickness of the boundary layer (mg g^{-1}).

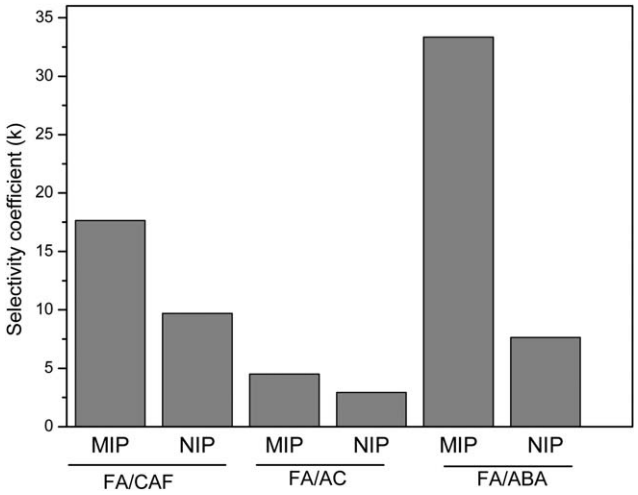

Figure 6. Selectivity coefficient for RAM-MIP and RAM-NIP in the presence of different competitors. FA, folic acid; CAF, caffeine; AC, acetaminophen; ABA, 4-aminobenzamide.

fragments of the folic acid molecule. As can be observed, the constants selectivity (k) for the RAM-MIP are larger than for the RAM-NIP, which indicates that even in the presence of a competitor molecule, the sorption of folic acid by RAM-MIP occurs in selective binding sites formed by the chemical imprinting.[40] These results give rise to relative selectivity coefficients (k') ($k' = k_{\text{RAM-MIP}}/k_{\text{RAM-NIP}}$) of 1.8, 1.5, and 4.4 for the competitive sorption FA/CA, FA/AC, and FA/ABA, respectively. These findings show the satisfactory molecular recognition, especially if one considers that the competitor molecules present smaller structure than the folic acid, and thus, it would be expected an easier mass transfer towards the binding sites owing to the absence of impeding steric effect.

Reusability of RAM-MIP

In order to assess the reusability of RAM-MIP a cartridge packed with 100.0 mg of RAM-MIP was percolated with 10.0 mL of folic acid solution followed by elution with 1.0 mL of the mixture acetonitrile:0.266 mol L^{-1} acetate buffer at pH 5.7 (15:85, v/v), the mobile phase of HPLC system. In this procedure, no washing step was required. The eluate was directly injected in the chromatographic system and the peak of folic acid at retention time of 8.42 min was monitored at λ_{max} 281 nm. This procedure can be repeated at least 120 times and the relative standard deviation (RSD) for measurements was found to be 4.8%, thus indicating the high reusability of material.

Swelling Analysis

Table III shows the swelling ratio (Sr) for the RAM-MIP, RAM-NIP, and MIP. The water uptake by the materials was found to be very high when compared with other hybrid material previously prepared,[29] which indicates the high hydrophilicity of the materials. The lower swelling ratio (Sr) observed for RAM-MIP regarding RAM-NIP may be attributed to its lower porosity. The influence of porosity on the water uptake has been previously reported in literature.[60] This finding may still be justified by observing the swelling ratio (Sr) values for the RAM-NIP

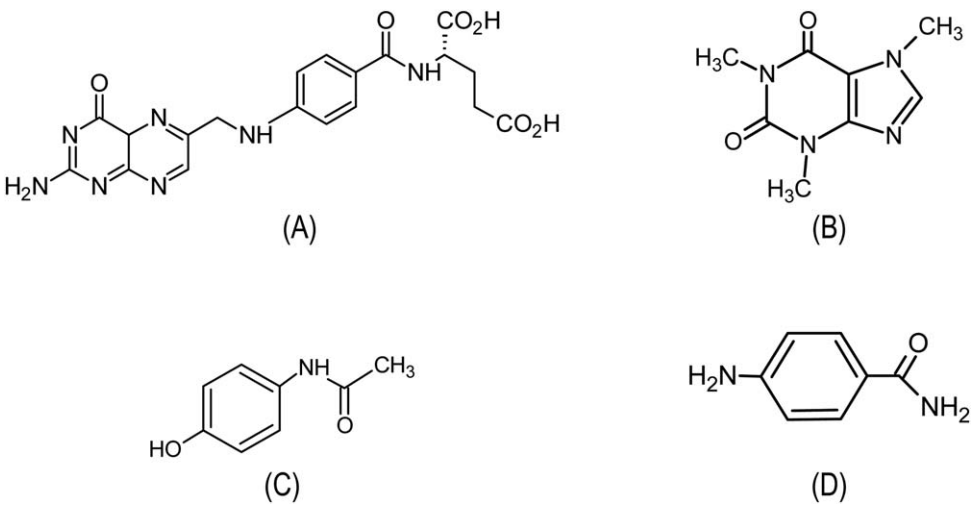

Figure 7. Molecular structures of (A) folic acid, (B) caffeine, (C) acetaminophen, and (D) 4-aminobenzamide.

Table III. Swelling Ratio Obtained for the Polymers

Polymer	Swelling ratio (%)
RAM-MIP	156.9 ± 3.2
RAM-NIP	230.0 ± 1.2
MIP	211.4 ± 4.8

and MIP compared to RAM-MIP. The latter polymer has lower swelling ratio and lower porosity. On the other hand, RAM-NIP and MIP have similar textural properties (Table I), but the water uptake by RAM-NIP was slight higher than MIP, which may be related to its more pronounced hydrophilic properties in relation to the MIP.

CONCLUSIONS

We have demonstrated for the first time the synthesis of a water-compatible hybrid molecularly imprinted polymer combined with restricted access for the selective recognition of folic acid. The selectivity data has confirmed that the hybrid material RAM-MIP is water-compatible and presents selectivity towards folic acid. The characterization by FTIR, TGA, TEM, and textural data were useful to confirm the polymerization of organic and inorganic fractions, obtaining mesoporous polymers and particles with high adhesion among themselves, acquiring morphological properties of monoliths. The kinetic studies showed that RAM-MIP has higher sorption of folic acid (5.6 mg g^{-1}) in relation to RAM-NIP (4.5 mg g^{-1}), and MIP (4.8 mg g^{-1}). The kinetic models of Elovich and pseudo-second order showed that the folic acid sorption occurs in sites with different binding energy. According with the intraparticle diffusion model, it was observed that the diffusion inside the pores is not the only process responsible for the retention of folic acid, indicating that sorption on the outer surface material also plays an important role on the folic acid retention. The thermodynamic parameters showed that the folic acid sorption in the material is of physical nature, besides demonstrating that the sorption process is exothermic and spontaneous. As a final remark, we believe that the proposed RAM-MIP herein synthesized has interesting features for solving the challenging problems of molecular recognition of MIPs in water medium even for large molecules as the folic acid.

ACKNOWLEDGMENTS

The authors would like to thank the Conselho Nacional de Desenvolvimento Científico e Tecnológico (CNPq) (Project No 481669/2013-2, 305552/2013-9, 472670/2012-3), Coordenação de Aperfeioamento de Pessoal de Nivel Superior (CAPES) (25/2014), Fundação Araucária do Paraná (163/2014) and Instituto Nacional de Ciência e Tecnologia de Bioanalítica (INCT) (Project No. 573672/2008-3) for their financial support and fellowships.

REFERENCES

1. Wulff, G.; Sarhan, A. *Angew. Chem. Int. Ed.* **1972**, *11*, 341.
2. Tarley, C. R. T.; Sotomayor, M. D. P. T.; Kubota, L. T. *Quim. Nova* **2005**, *28*, 1076.
3. Tarley, C. R. T.; Sotomayor, M. D. P. T.; Kubota, L. T. *Quim. Nova* **2005**, *28*, 1087.
4. Cheong, W. J.; Yang, S. H.; Ali, F. *J. Sep. Sci.* **2013**, *36*, 609.
5. Puoci, F.; Cirillo, G.; Curcio, M.; Parisi, O. I.; Iemma, F.; Picci, N. *Expert. Opin. Drug. Deliv.* **2011**, *8*, 1379.
6. Wulff, G.; Liu, J. *Acc. Chem. Res.* **2012**, *45*, 239.
7. Sartori, L. R.; Santos, W. J. R.; Kubota, L. T.; Segatelli, M. G.; Tarley, C. R. T. *Mater. Sci. Eng. C* **2011**, *31*, 114.
8. Parisi, O. I.; Cirillo, G.; Curcio, M.; Puoci, F.; Iemma, F.; Spizzirri, U. G.; Picci, N. *J. Polym. Res.* **2010**, *17*, 355.
9. Zhao, M.; Chen, X.; Zhang, H.; Yan, H.; Zhang, H. *Biomacromolecules* **2014**, *15*, 1663.
10. Haginaka, J. *J. Sep. Sci.* **2009**, *32*, 1548.
11. Boos, K. S.; Fleischer, C. T. *Fresenius J. Anal. Chem* **2001**, *371*, 16.
12. Sanbe, H.; Hoshina, K.; Haginaka, J. *J. Chromatogr. A* **2007**, *1152*, 130.
13. Hall, A. J.; Quaglia, M.; Manesiotis, P.; De Lorenzi, E.; Sellergren, B. *Anal. Chem.* **2006**, *78*, 8362.

14. Díaz-Garcia, M. E.; Laínño, R. B. *Microchim. Acta* **2005**, *149*, 19.
15. Gupta, R.; Kumar, A. *Biotechnol. Adv.* **2008**, *26*, 533.
16. Pereira, A. V.; Cervini, P.; Cavalheiro, E. T. G. *Anal. Methods* **2014**, *6*, 6658.
17. Dickert, F. L.; Hayden, O. *Adv. Mater.* **2000**, *12*, 311.
18. Dirion, B.; Cobb, Z.; Schillinger, E.; Anderson, L. I.; Sellergren, B. *J. Am. Chem. Soc.* **2003**, *125*, 15101.
19. Sanbe, H.; Haginaka, J. *Analyst* **2003**, *128*, 593.
20. Haginaka, J.; Takehira, H.; Hosoya, K.; Tanaka, N. *J. Chromatogr. A* **1999**, *849*, 331.
21. Poncin-Epaillard, F.; Vrlinic, T.; Debarnot, D.; Mozetic, M.; Coudreuse, A.; Legeay, G.; Moualij, B. E.; Zorzi, W. *J. Funct. Biomater.* **2012**, *3*, 528.
22. Puoci, F.; Iemma, F.; Cirillo, G.; Curcio, M.; Parisi, O. I.; Spizzirri, U. G.; Picci, N. *Eur. Polym. J.* **2009**, *45*, 1634.
23. Clausen, D. N.; Pires, I. M. R.; Tarley, C. R. T. *Mater. Sci. Eng. C* **2014**, *44*, 99.
24. Tarley, C. R. T.; Andrade, F. N.; Oliveira, F. M.; Corazza, M. Z.; Azevedo, L. F. M.; Segatelli, M. G. *Anal. Chim. Acta* **2011**, *703*, 145.
25. Lv, T. K.; Wang, L. M.; Yang, L.; Zhao, C. X.; Sun, H. W. *J. Chromatogr. A* **2012**, *1227*, 48.
26. Yan, H.; Wang, M.; Han, Y.; Qiao, F.; Row, K. H. *J. Cromatogr. A* **2014**, *1346*, 16.
27. Clausen, D. N.; Visentainer, J. V.; Tarley, C. R. T. *Analyst* **2014**, *139*, 5021.
28. Lin, C. I.; Joseph, A. K.; Chang, C. K.; Wang, U. C.; Lee, Y. D. *Anal. Chim. Acta* **2003**, *481*, 175.
29. Lv, Y. K.; Wang, L. M.; Yang, S. L.; Wang, X. H.; Sun, W. H. *J. Appl. Polym. Sci.* **2012**, *126*, 1631.
30. Quaglia, M.; Chenon, K.; Hall, A. J. D.; Lorenzi, E.; Sellergren, B. *J. Am. Chem. Soc.* **2001**, *123*, 2145.
31. Karimian, N.; Zavar, M. H. A.; Chamsaz, M.; Turner, A. P. F.; Tiwari, A. *Electrochem. Commun.* **2013**, *36*, 92.
32. Prasad, B. B.; Tiwari, M. P.; Madhuri, R.; Sharma, P. S. *Anal. Chim. Acta* **2010**, *662*, 14.
33. Hussain, M.; Iqbal, N.; Lieberzeit, P. A. *Sens. Act. B* **2013**, *176*, 1090.
34. Kotova, K.; Hussain, M.; Mustafa, G.; Lieberzeit, P. A. *Sens. Act. B* **2013**, *189*, 199.
35. Jin, Y.; Jiang, M.; Shi, Y.; Lin, Y.; Peng, Y.; Dai, K.; Lu, B. *Anal. Chim. Acta* **2008**, *612*, 105.
36. Yeh, J.-M.; Weng, C.-J.; Liao, W.-J.; Mau, Y.-W. *Surf. Coat. Technol.* **2006**, *201*, 1788.
37. Du, B.; Qu, T.; Chen, Z.; Cao, X.; Han, S.; Shen, G.; Wang, L. *Talanta* **2014**, *129*, 465.
38. Tarley, C. R. T.; Andrade, F. N.; Santana, H.; Zaia, D. A. M.; Beijo, L. A.; Segatelli, M. G. *React. Funct. Polym.* **2012**, *72*, 83.
39. Nekouei, F.; Nekouei, S.; Tyagi, I.; Gupta, V. K. *J. Mol. Liq.* **2015**, *201*, 24.
40. Oliveira, F. M.; Somera, B. F.; Ribeiro, E. S.; Segatelli, M. G.; Yabe, M. J. S.; Galunin, E.; Tarley, C. R. T. *Ind. Eng. Chem. Res.* **2013**, *52*, 8550.
41. Parameswaran, G.; Mathew, B. *Adv. Environ. Chem* **2014**, *2014*, 1.
42. Liu, Y.-L.; Su, Y.-H.; Lai, J.-Y. *Polymer* **2004**, *45*, 6831.
43. Liu, B.; Yan, E.; Zhang, X.; Yang, X.; Bai, F. *J. Colloids Interface Sci.* **2012**, *369*, 144.
44. Archer, P. D. J.; Ming, D. W.; Sutter, B. *Planet. Sci.* **2013**, *2*, 1.
45. Vélez, J. F.; Procaccini, R. A.; Aparicio, M.; Mosa, J. *Electrochim. Acta* **2013**, *110*, 200.
46. Macan, J.; Brnardic, I.; Orlic, S.; Ivankovic, H.; Ivankovic, M. *Polym. Degrad. Stabil.* **2006**, *91*, 122.
47. Zhang, Y.; Zhang, Y.; Zhang, H. *Braz. J. Chem. Eng* **2008**, *25*, 201.
48. Zu, L.; Li, R.; Jin, L.; Lian, H.; Liu, Y.; Cui, X. *Prog. Nat. Sci.* **2014**, *24*, 42.
49. Ponyrko, S.; Kobera, L.; Brus, J.; Matejka, L. *Polymer* **2013**, *54*, 6271.
50. Renkecz, T.; Mistlberger, G.; Pawlak, M.; Horváth, V.; Bakker, E. *Appl. Mater. Interfaces* **2013**, *5*, 8537.
51. Cormack, P. A. G.; Elorza, A. Z. *J. Chromatogr. B* **2014**, *804*, 173.
52. Ibarra-Montaño, E. L.; Rodríguez-Laguna, N.; Sánchez-Hernández, A.; Rojas-Hernández, A. *J. Appl. Sol. Chem. Model* **2015**, *4*, 7.
53. Yu, Q.; Deng, S.; Yu, G. *Water Res.* **2008**, *42*, 3089.
54. Lopez, M. M. C.; Perez, M. C. C.; Garcia, M. S. D.; Vilariño, J. M. L.; Rodriguez, M. V. G.; Losada, L. F. B. *Anal. Chim. Acta* **2012**, *721*, 68.
55. Zhou, C.; Wu, Q.; Lei, T.; Negulescu, I. I. *Chem. Eng. J.* **2014**, *251*, 17.
56. Cheung, W. H.; Szeto, Y. S.; McKay, G. *Bioresource Technol.* **2007**, *98*, 2897.
57. Carvalho, T. E. M.; Fungaro, D. A.; Izidoro, J. C. *Quim. Nova* **2010**, *33*, 358.
58. Xue, Y.; Hou, H.; Zhu, S. *Chem. Eng. J.* **2009**, *147*, 272.
59. Site, A. D. *J. Phys. Chem. Ref. Data* **2001**, *30*, 187.
60. Wu, N.; Sun, Y.; Jiao, Y.; Chen, L. *J. Eng. Fiber. Fabr* **2013**, *8*, 1.